Supplementary Material (ESI) for Organic & Biomolecular Chemistry

SUPPORTING INFORMATION

Docking, Synthesis, and NMR Studies of Mannosyl Trisaccharide Ligands for DC-SIGN Lectin

José J. Reina,[a] Irene Díaz,[a] Pedro M. Nieto,*[a] Nuria E. Campillo,[b] Juan A. Páez,[b] George Tabarani,[c] Franck Fieschi,[c] and Javier Rojo*[a]

A.- DOCKING

A.1 Structural parameters of selected solutions.

Disaccharide Manα(1-3)Man

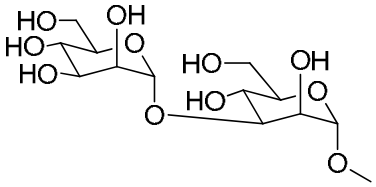

Figure S1. *Representation of the relationship between dihedral angles Psi/Phi corresponding to the different docking solution of dissacharide Manα(1-3)Man*

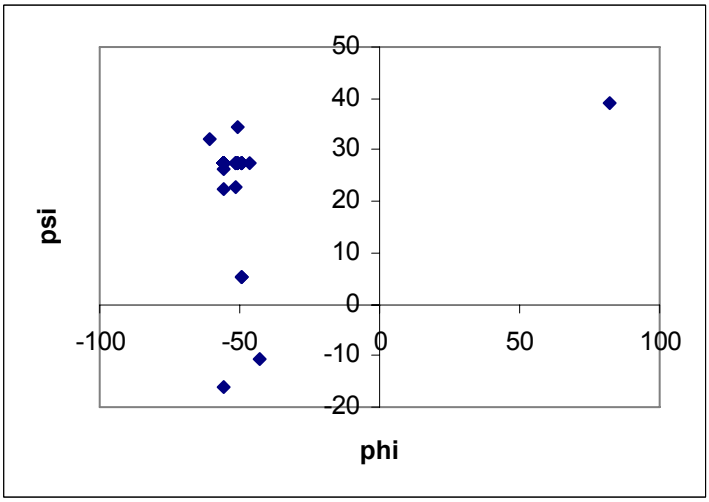

Figure S2*. The relationship between the proton distance H1aH3d/H1aH2d of the docking solutions corresponding to the dissacharide Manα(1-3)Man are shown in the diagram*

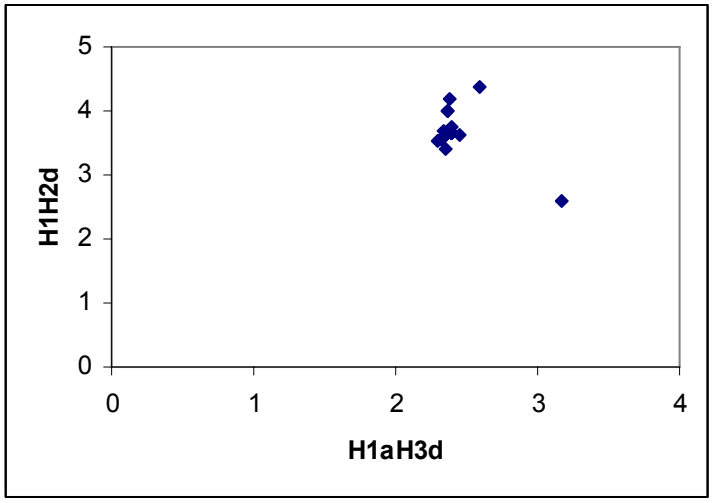

Figure S3. *Representation of the distance (Å) from atom O3 of the dissacharide Manα(1-3)Man to ion Ca^{2+} for each docking solution*

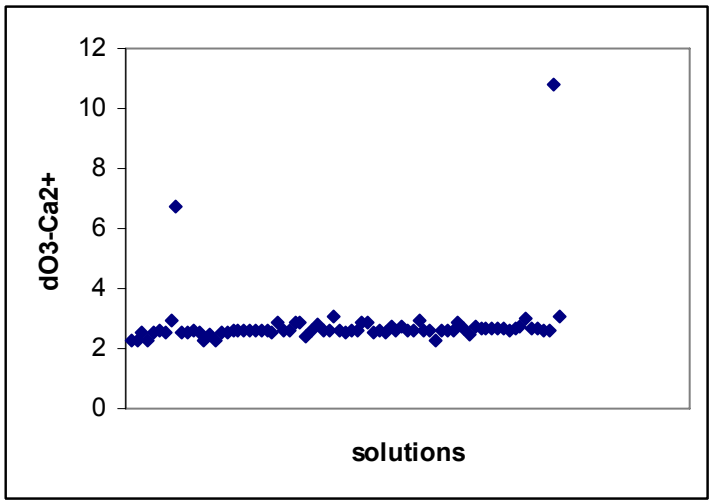

Figure S4*. Proposed binding modes for dissacharide Manα1,3Man with DC-SIGN. The calcium ion is represented by a magenta sphere. Sticks representation for each binding mode of the dissacharide are shown*

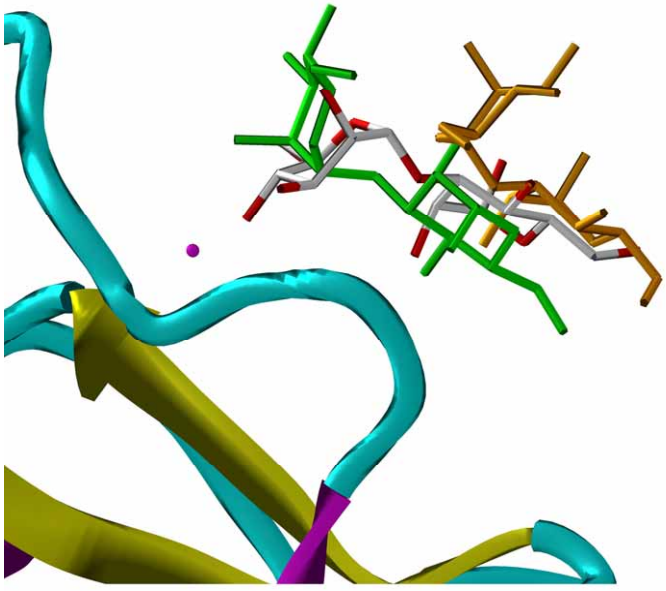

Disaccharide Manα(1-2)Man

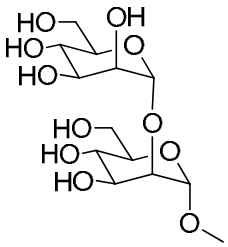

***Figure S5**. Representation of the relationship between dihedral angles Psi/Phi corresponding to the different docking solution of dissacharide Manα(1-2)Man*

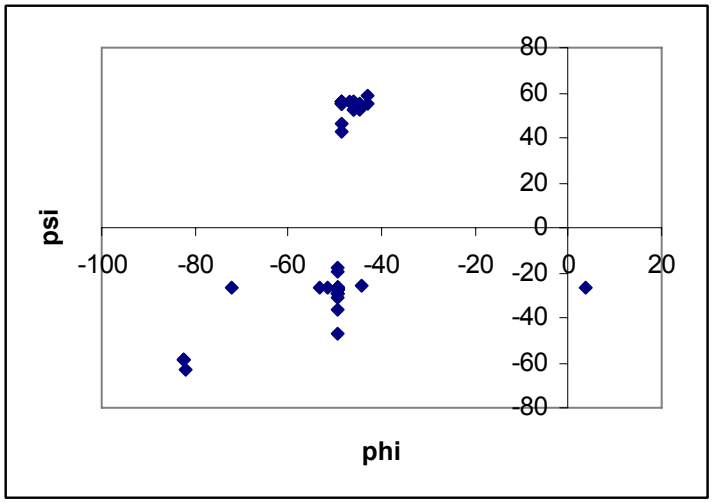

***Figure S6.** The relationship between the proton distance H1cH1a/H1cH2a of the docking solutions corresponding to the dissacharide Manα(1-2)Man are shown in the diagram*

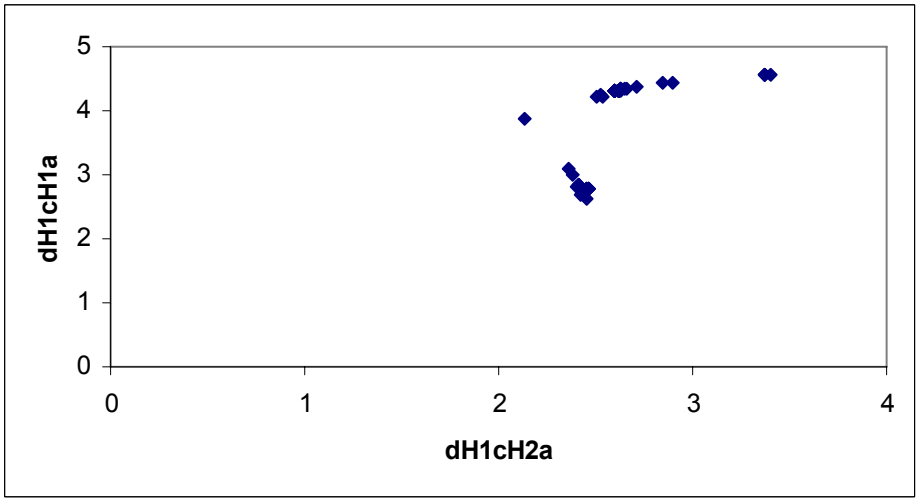

***Figure S7**. Representation of the distance (Å) from atom O3 of the dissacharide Manα(1-2)Man to ion Ca^{2+} for each docking solution.*

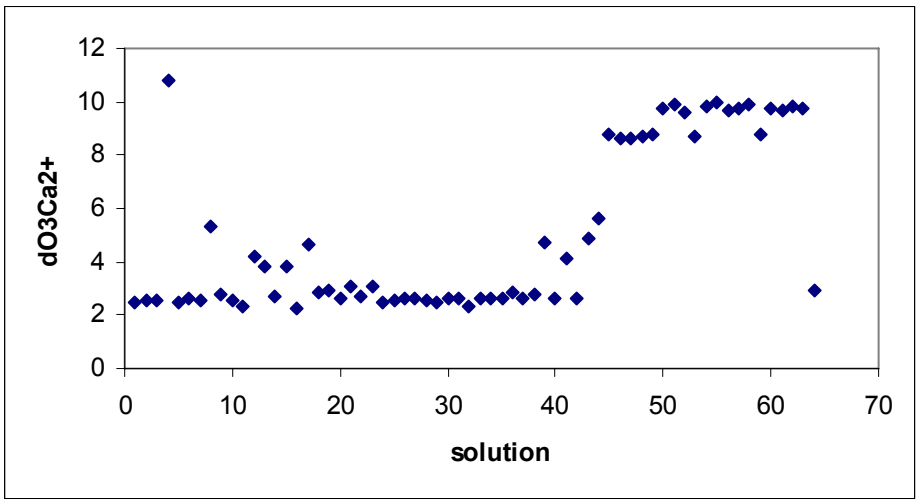

***Figure S8** Proposed binding modes for dissacharide Manα(1,2)Man with DC-SIGN. The calcium ion is represented by a magenta sphere. Sticks representation for each binding mode of the dissacharide are shown. The minor orientation (reducing end that bounds the Ca^{2+}) is shown in orange colour*

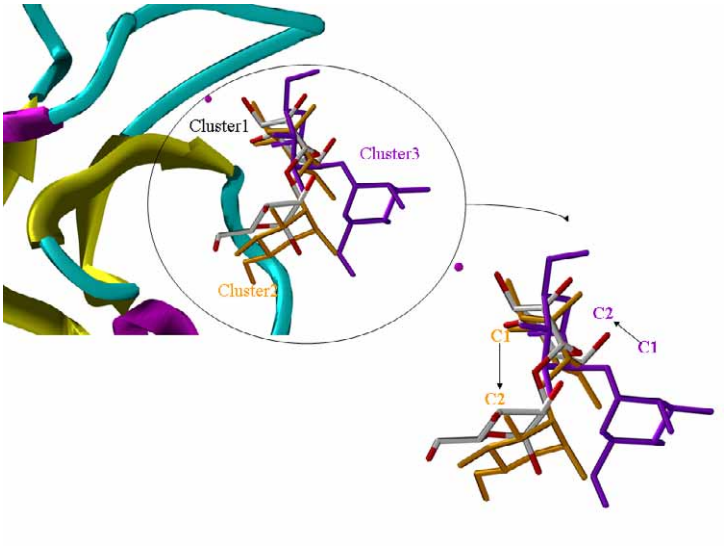

Disaccharide Manα(1-6)Man

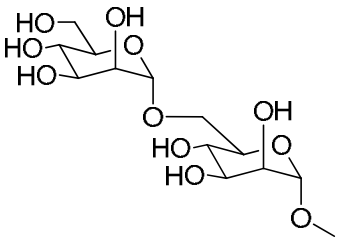

Figure S9. *Representation of the relationship between dihedral angles Psi/Phi corresponding to the different docking solution of dissacharide Manα(1-6)Man.*

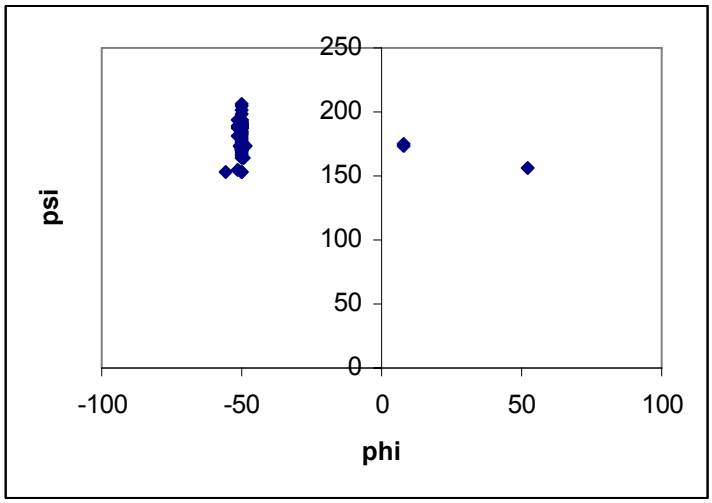

Figure S10. *The relationship between the proton distance H1bH6´´a/ H1bH6´a of the docking solutions corresponding to the dissacharide Manα(1-6)Man are shown in the diagram*

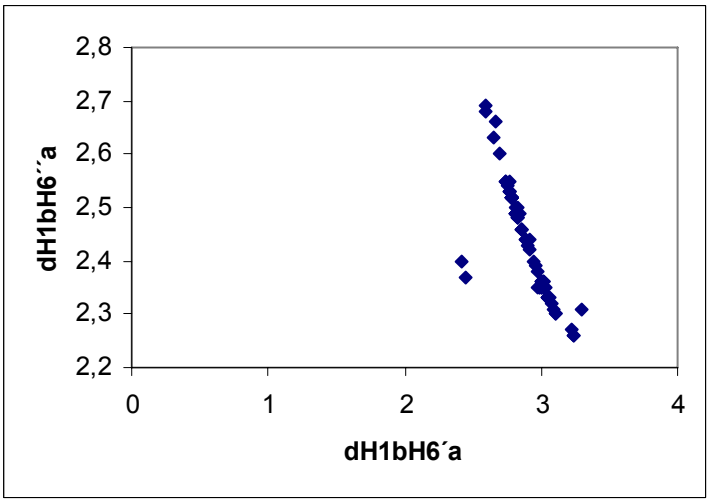

Figure S11. *Representation of the distance (Å) from atom O3 of the dissacharide Manα(1-6)Man to ion Ca^{2+} for each docking solution*

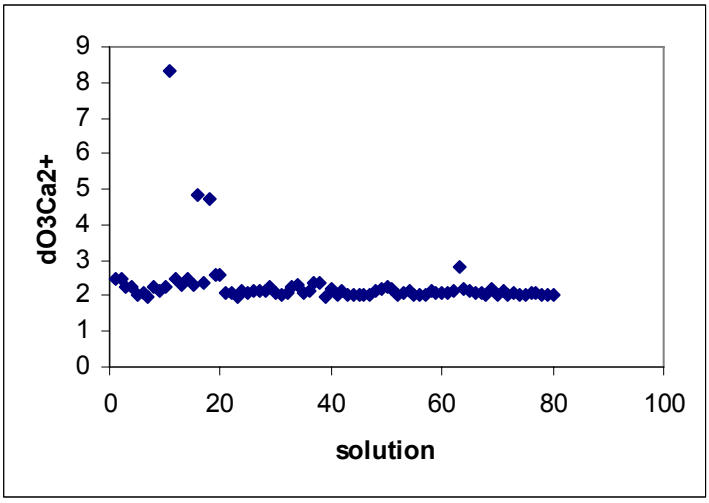

Figure S12. *Proposed binding modes for dissacharide Manα(1,2)Man with DC-SIGN. The calcium ion is represented by a magenta sphere. Sticks representation for each binding mode of the dissacharide are shown*

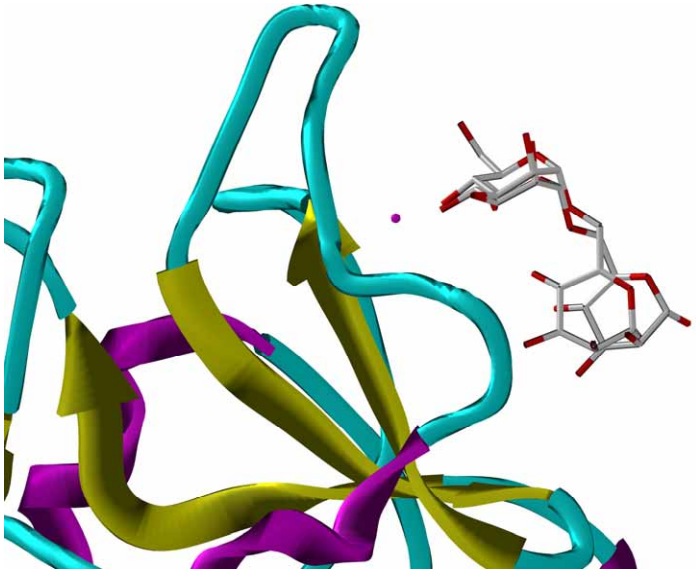

Trisaccharide Manα1,3[Manα1-6]Man

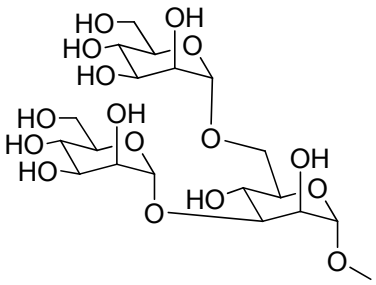

Figure S13. *Representation of the relationship between dihedral angles Psi/Phi of Manα1,3 moiety corresponding to the different docking solution of trissacharide Manα1,3[Manα1-6]Man*

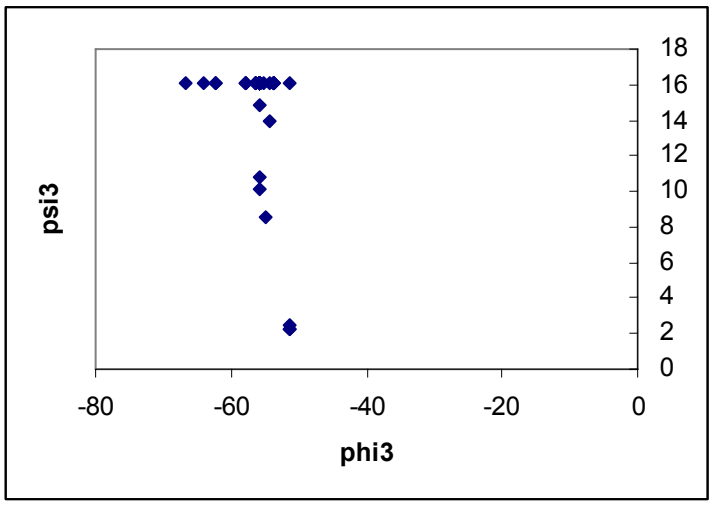

Figure S14. *The relationship between the proton distance H1aH2d/ H1aH3d of the docking solutions corresponding to Manα1,3 moiety the trissacharide Manα1,3[Manα1-6]Man are shown in the diagram*

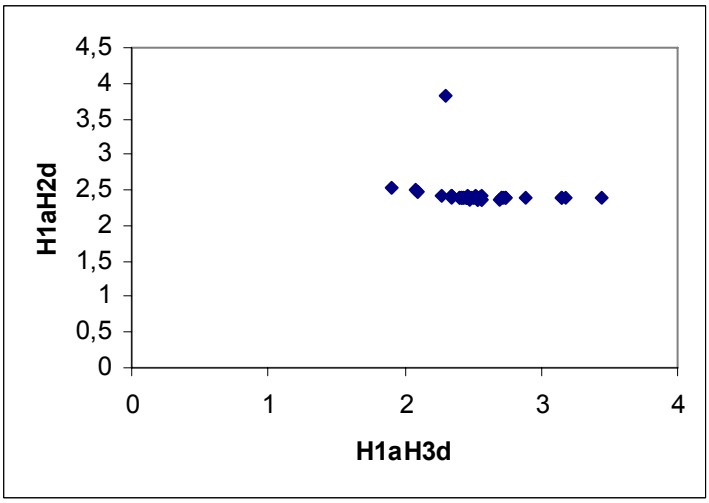

Figure S15. *Representation of the relationship between dihedral angles Psi/Phi of Manα1,6 moiety corresponding to the different docking solution of trissacharide Manα1,3[Manα1-6]Man*

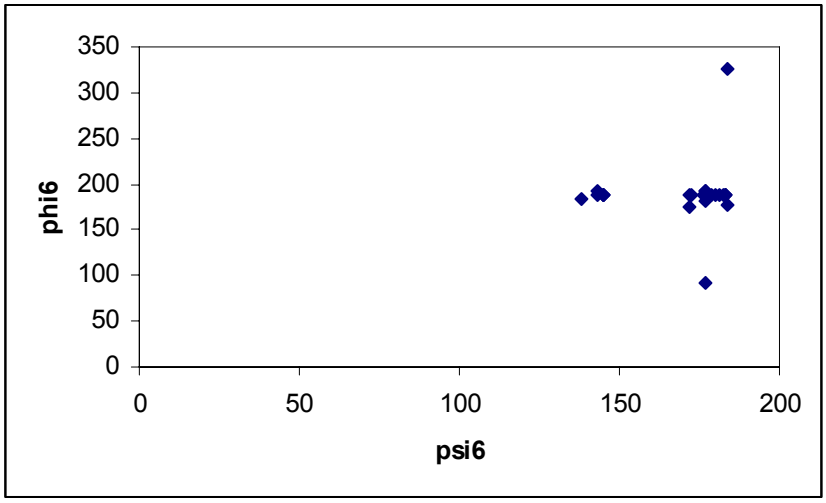

Figure S16. *The relationship between the proton distance H1b-H6´a/ H1b-H6´´ a of the docking solutions corresponding to Manα1,6 moiety the trissacharide Manα1,3[Manα1-6]Man are shown in the diagram*

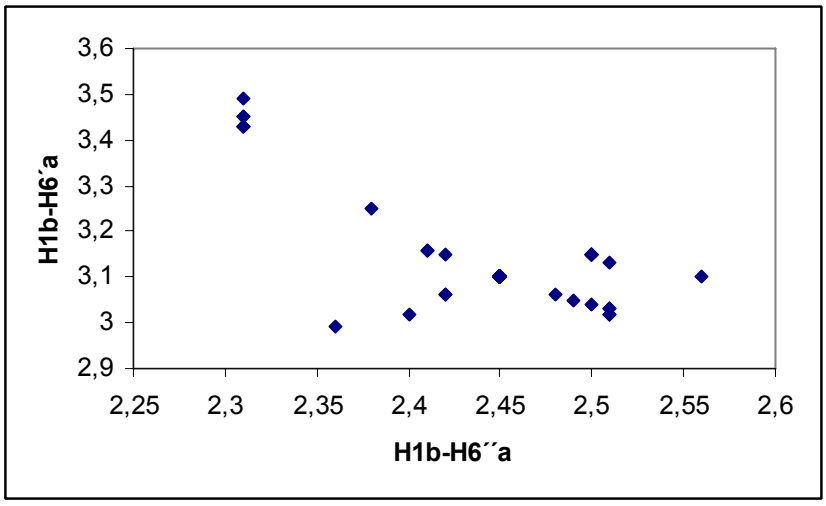

Figure S17. *Ribbon representation of the structural superposition of the docking complex Manα1,3[Manα1,6]Man with DC-SIIGN and X-Ray structure1k9i. Sticks representation for each ligand are shown. The ligand GlcNAC2MAN3 (1k9i) is shown in magenta colour. The calcium ion is represented by a magenta sphere.*

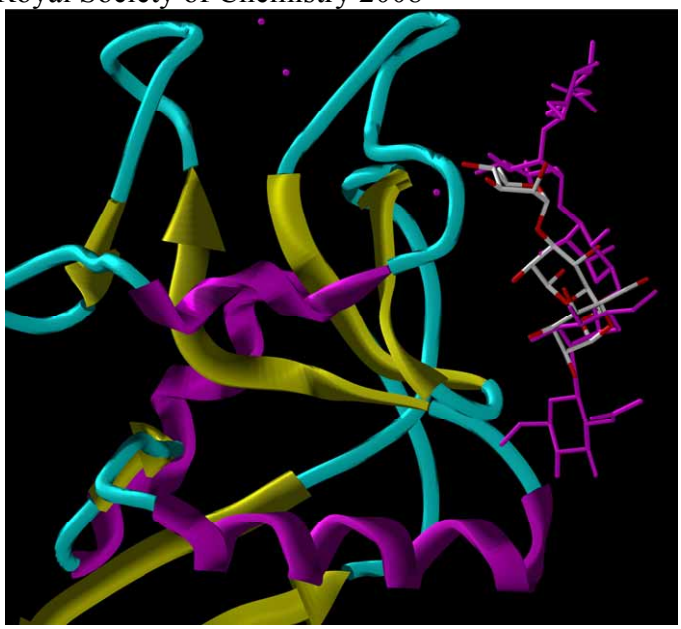

Trisaccharide Manα1,2[Manα1-6]Man

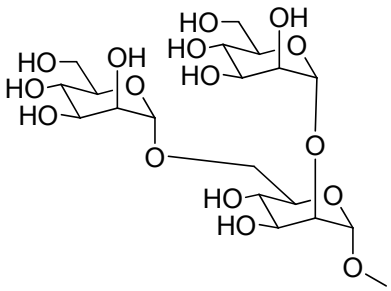

Figure S18. *Representation of the relationship between dihedral angles Psi/Phi of Manα1,2 moiety corresponding to the different docking solution of trissacharide Manα1,2[Manα1-6]Man*

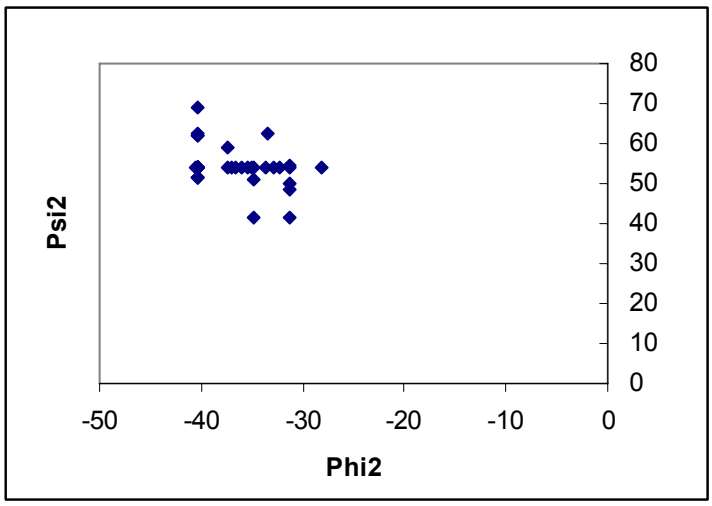

Figure S19. *The relationship between the proton distance H1cH2a/ H1cH1a of the docking solutions corresponding to Manα1,2 moiety the trissacharide Manα1,2[Manα1-6]Man are shown in the diagram*

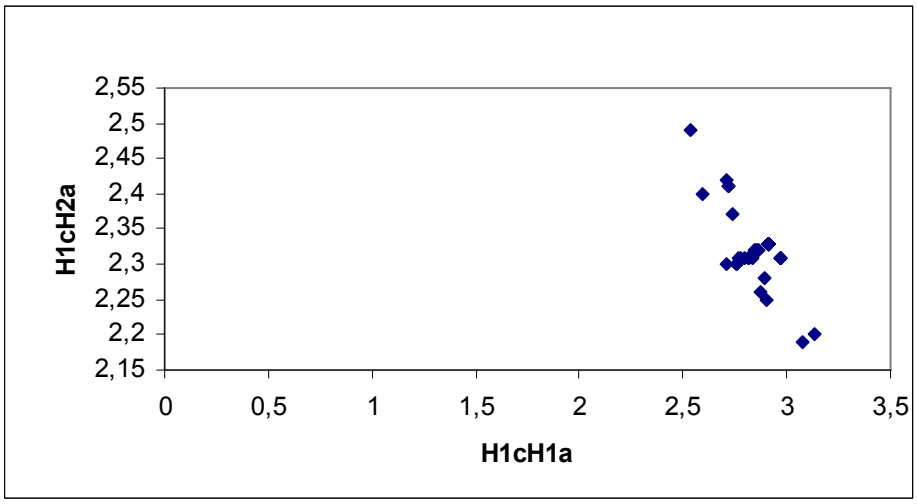

Figure S20. *Representation of the distance (Å) from atom O3 of the trissacharide Manα1,2[Manα1-6]Man ion Ca^{2+} for each docking solution*

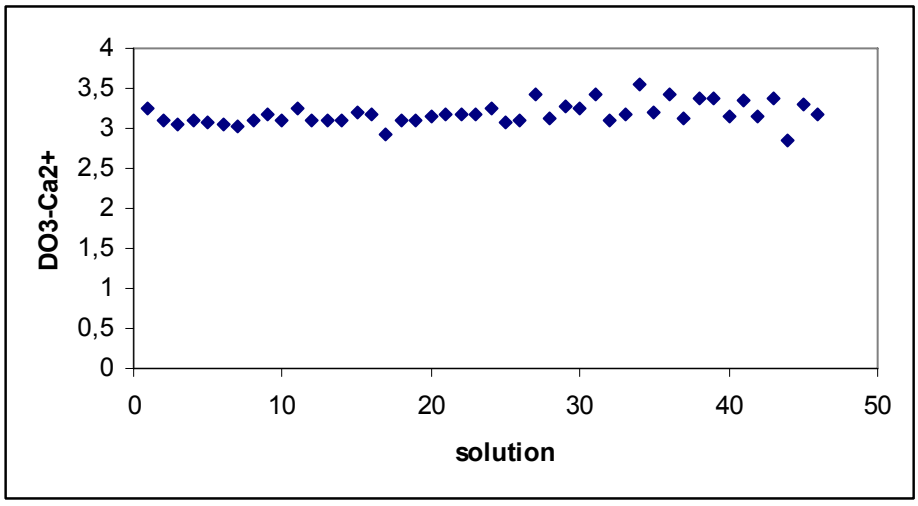

Figure S21. *Representation of the relationship between dihedral angles Psi/Phi of Manα1,6 moiety corresponding to the different docking solution of trissacharide Manα1,2[Manα1-6]Man*

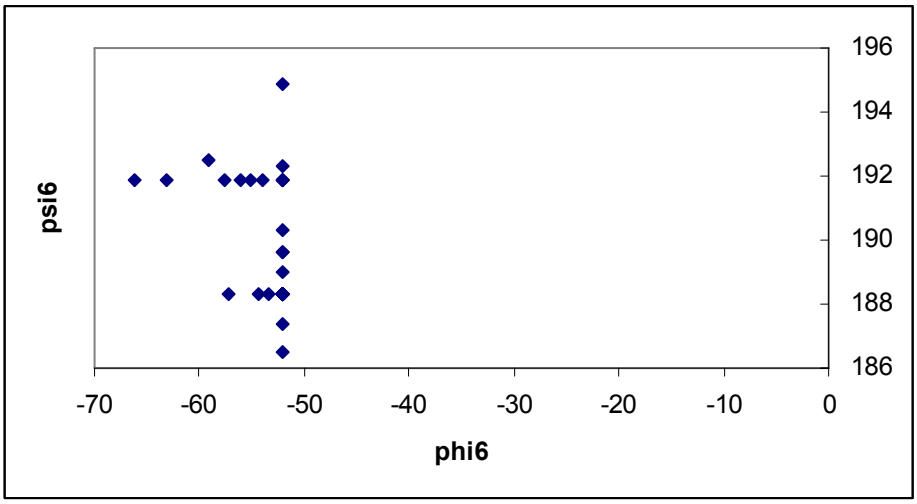

Figure S22 *The relationship between the proton distance H1bH16´´/ H1b-H16´ of the docking solutions corresponding to Manα1,6 moiety the trissacharide Manα1,2[Manα1-6]Man are shown in the diagram*

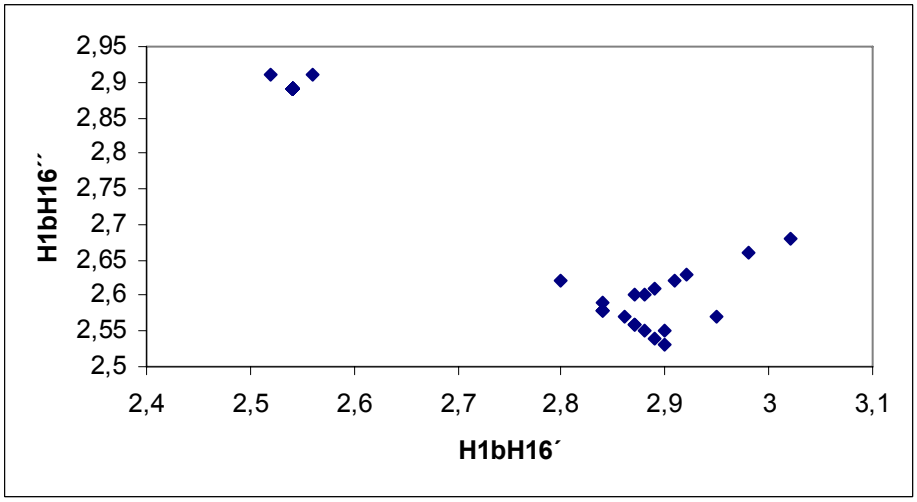

A.2 Analysis of Docking solutions. Protein-Ligand interactions.

The final complexes (1d13, 1d16, 2d16, 1d12, 2d12, 1t36 and 1t26) were evaluated in terms of consensus of ligand-protein interactions. Careful analysis of such complexes interactions led to identification of the key protein residues involved in the binding sites and to propose the hydrogen bond network gathered in Table S1.

Dimannosides

As depicted in Table S1, a large number of hydrogen bond stabilizing interactions between the mannose units and DC-SIGN contribute to the energetically favoured status of complexes 1d16 and 1d12. These hydrogen bonds, which are also present in the complex 1d13 of the disaccharide Manα1,3Man (Table S1), were experimentally observed in the complex of DC-SIGN and the pentasaccharide $GlcNAc_2Man_3$ (see Table S1). The strongest interactions were encountered between the rings ManD in dimannoside 1d13, ManB in 1d16 and ManC in 1d12 through the residues Glu 347, Asn 349, Glu 354, Asn 365, Asp 366 and Lys 368, which constitute the primary binding site. In addition to these interactions, the equatorial 3- and 4-hydroxyl groups of each disaccharide are bound to the Ca^{2+} ion (see Table S1), which is also supported by the experimental data. Other remarkable interactions are the hydrophobic contacts of the cyclohexose ring of ManA with Val 351 and Phe 313. The complexes 1d16 and 1d12 show stacking between the ManA unit and the aromatic residue Phe 313. Moreover, the mannose ManA in complex 1d12 shows a C-H$\cdots$aromatic interaction (α_{chx}= 155.4, d_{CX} (Å) = 4.3, d_{HpX} (Å) = 2.4). The ΔG_{bind} and the docking energy calculated with STC and DOCK program respectively, suggest that the disaccharides with α1-2 and α1-6 type union are the best ligands for DC-SIGN (Table 1).

Trimannosides

The structural parameters of the final complex of each trissacharide and the energy of interaction are gathered in Table S1. The hydrogen bond network mentioned before for the disaccharides is preserved in both trisaccharide-complex models, along with some additional hydrogen bonds observed for ManB in Manα1,2[Manα1,6]Man complex. Both trisaccharides show hydrophobic interaction between the ManC (1t26) and ManD (1t36) units and the Val 351 residue. Aromatic interactions of both complexes with Phe 313 have also been found. In addition, the mannose ManA in Manα1,2[Manα1,6]Man complex displays a C-H$\cdots$aromatic interaction ($\alpha_{ch\,x}$= 160.2, d_{CX} (Å) = 4.0, d_{HpX} (Å) = 1.2).

Table S1. *Potential hydrogen bonds.*

Complex	*Hydrogen bond* (Å)		
1k9i	**Man 1→**	**3 Man 6**	**←1 Man**
	Glu 347/O3 (2.8)		Ser 360/O3 (2.9)
	Glu 354/O4 (2.4		Asn 344/O3 (3.9)
	Asn 365/O4 (2.9)	-	
	Asp 367/O6 (3.5		
	Ca/O3,O4 (2.6 ,2.7)		
2it6	**Man 1→**	**2 Man**	
	Glu 358/O3 (2.7)	Glu 347/O4 (3.1)	
	Ser 360/O3 (2.7)	Glu 347/O6 (2.7)	
	Ser 360/O4 (3.2)	Glu 349/O4 (2.8)	
	Asn 367/O2 (3.5)	Glu 354/O3 (2.4)	
	Lys 373/O2 (3.8)	Asn 365/O3 (2.9)	
		Asp 366/O3(2.8)	
		Lys 368/O1(4.5)	
		Ca/O3,O4 (2.5, 2.5)	
1d13	**Man 1(Man D)→**	**3 Man(Man A)**	
	Glu 347/O3 (2.8)		
	Asn 349/O3 (2.6)		
	Glu 354/O4 (2.6)		
	Asn 365/O4 (2.9)	-	-
	Asp 366/O4 (2.6)		
	Asp 367/O6 (3.7)		
	Ca/O3,O4 (2.7 ,2.8)		
1d16	**Man 1(Man B)→**	**6 Man(Man A)**	
	Glu 347/O3 (2.9)	Ser 360/O4 (2.9)	
	Asn 349/O3 (3.1)		
	Glu 354/O4 (2.7)		
	Asn 365/O4 (3.4)		-
	Asp 366/O4 (3.0)		
	Asp 367/O6 (2.8)		
	Ca/O3,O4 (2.8 ,2.8)		
2d16		**Man 6(Man A)**	**←1 Man(Man B)**
			Asn 344/O3 (3.7)
	-	-	Ser 360/O3 (3.0)
			Gly 361/O2 (3.7)
1d12	**Man 1(Man C)→**	**2 Man(Man A)**	
	Glu 354/O4 (2.6)	Glu 358/O4 (2.9)	
	Asn 365/O4 (3.3)	Ser 360/O5 (3.1)	
	Asp 366/O4 (3.6)	Ser 360/O1 (3.5)	-
	Lys 368/O4 (2.9)	Asn 365/O5 (3.4)	
	Ca/O3,O4 (4.4, 2.9)		
2d12		**Man 2(Man C)**	**←1 Man(Man A)**
		Ser 360/O2 (3.2)	Asn 344/O3 (3.1)
		Ser 360/O5 (3.7)	Ser 360/O3 (3.0)
	-	Asn 365/O5 (3.6)	
		Asp 367/O6 (3.4)	
		Lys 373/O6 (3.4)	
1t36	**Man 1 (ManD)→**	**3 Man 6(ManA)**	**←1 Man(ManB)**
	Glu 347/O3 (2.9)		Asn 344/O3 (3.6)
	Asn 349/O3 (3.3)		Ser 360/O3 (2.9)
	Glu 354/O4 (2.6)	-	Arg 345/O4 (2.8)
	Asn 365/O4 (3.3)		
	Asp 366/O4 (3.0)		
	Asp 367/O6 (2.8)		
	Ca/O3,O4 (2.8 ,2.9)		
1t26	**Man 1 (ManC)→**	**2 Man 6(ManA)**	**←1 Man(ManB)**
	Glu 347/O3 (3.0)		Glu 358/O3 (2.7)
	Asn 349/O2 (2.8)		Ser 360/O4 (2.9)
	Glu 354/O4 (2.7)	-	Asn 365/O3 (3.0)
	Asn 365/O4 (3.2)		Asp 367/O3 (3.7)
	Lys 368/O6 (2.9)		Lys 373/O3 (2.9)
	Ca/O3,O4 (2.8, 3.0)		

B.- NMR

B.1 CONFORMATIONAL ANALYSIS.

For comparison purposes, bound data were compared with additional NMR data for the compounds in absence of protein registered in the same experimental conditions as used for the studies of the complexes with DC-SIGN. Although the conformational analysis of these trisaccharides have been performed by other authors, this measurements were performed in order to verify that no minor conformational change was due to the high salt concentration required to stabilize the protein. The experimental distances obtained by NMR for **1** and **2** in presence of the same buffer and salt concentration as the used for the bound studies (Experiments registered at 500 MHz, in 150 mM NaCl, 20 mM TRIS-d_6 4 mM $CaCl_2$ at 278 K) agree with previous descriptions of this linkage. The results estimated by the bound conformation agree with the free compound indicating no conformational changes due to binding.

*Trisaccharide Manα1,2[Manα1,6]Man **1**.*

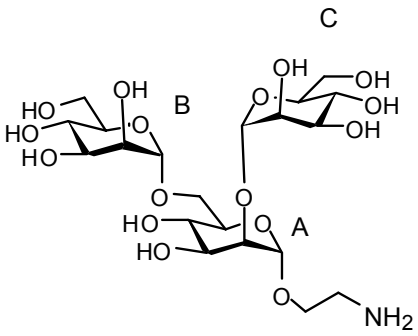

Figure S23 *NOE growing curves of **1**, free (left) and in presence of 1:20 molar of DC-SIGN (right). Experiments registered at 500 MHz, in 150 mM NaCl, 20 mM TRIS-d_6 4 mM $CaCl_2$ at 278 K using a mixing time of 600 ms for free and 400 ms in presence of DC-SIGN.*

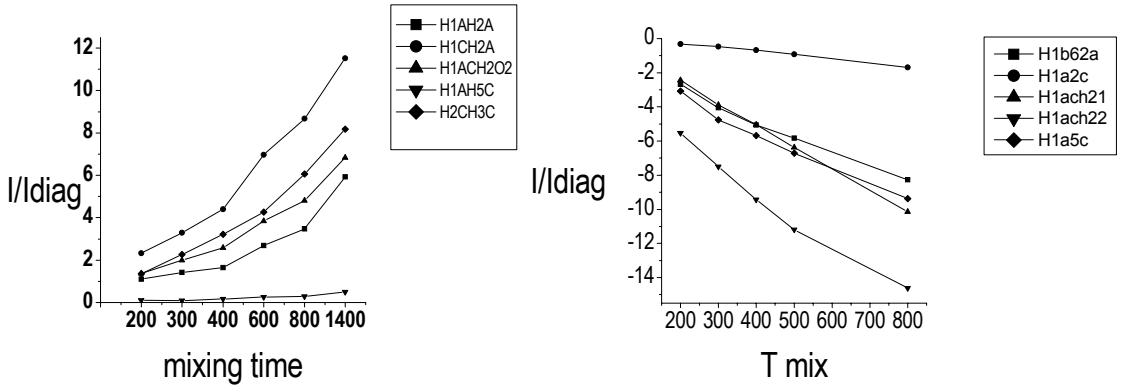

Table S2*. Interprotonic distances calculated from NOE growing rates for* ***1****, from the <r^{-6}> averaged distances along the MD simulations, and from the bound conformation obtained from docking for* ***1****. Fixed internal distances are included to verify the accuracy of the experimental distances.*

	Experimental NMR		**Theoretical**
	Free	**Bound**	**Docking**
1a2a	2.5	2.5	2.6
1a2c	nd	3.5	4.9
1a5c	3.7	2.6	3.2
1b3b	3.9	3.4	3.7
1b5b	3.7	3.6	3.7
1b6'a	3.9	3.8	2.7
1b6''a	2.5	2.6	2.4
1c1a	-	-	2.9
1c2a	2.3	2.5	2.3
2c3c	2.3	2.5	2.4

Trisaccharide Manα1,3[Manα1,6]Man **2**.

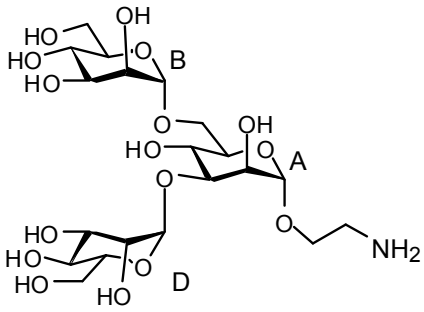

Figure S24. *NOE growing curves of* ***2****, free (left) and in presence of 1:20 molar of DC-SIGN (rigth). Experiments registered at 500 MHz, in 150 mM NaCl, 20 mM TRIS-d_6 4 mM $CaCl_2$ at 278 K using a mixing time of 600 ms for free and 400 ms in presence of DC-SIGN.*

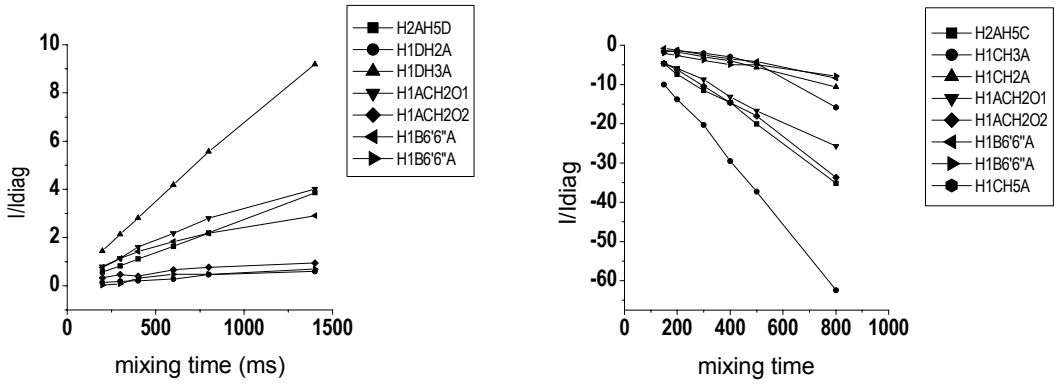

***Table S3**. Interprotonic distances calculated from NOE growing rates, for **2** from the $\langle r^{-6} \rangle$ averaged distances along the MD simulations, and from the bound conformation obtained from docking for **2**. Fixed internal distances are included to verify the accuracy of the experimental distances.*

	Experimental NMR		**Theoretical**
	Free	**Bound**	**Docking**
1a2a	2.5	2.5	2.6
1a5a	3.8	3.2	3.6
2a3a	2.4	2.4	2.4
2a5d	2.6	2.4	3.5
1b3b	3.3	3.5	3.7
1b5b	nd	3.0	3.7
1b6'a	3.7	3.5	2.9
1b6''a	2.5	2.8	2.4
1d2a	3.5	3.1	2.8
1d3a	2.3	2.2	2.1